

Effect of boron dimers on the superconducting critical temperature in boron-doped diamond

Břetislav Šopík^{a,b}, Pavel Lipavský^{a,b}

^a*Faculty of Mathematics and Physics, Charles University, Ke Karlovu 3, 12116 Prague 2, Czech Republic*

^b*Institute of Physics, Academy of Sciences, Cukrovarnická 10, 16253 Prague 6, Czech Republic*

Abstract

We study how attractive boron correlations in boron-doped diamond affect the superconducting critical temperature. The critical temperature is obtained from the McMillan formula for strong coupling superconductors with the density of states evaluated in the dynamical cluster approximation. Numerical results for the cluster of $2 \times 2 \times 2$ atoms show that attractive correlations lower the density of states at the Fermi level. We argue that this might explain experimentally observed differences in critical temperatures of 100 and 111 oriented films.

Keywords: diamond, boron, superconductivity, disorder, correlations, dimers

1. Introduction

Diamond is a typical insulator with a band gap of ~ 5.5 eV. It has been intensively studied for a long time due to its compatibility with human tissues and unique physical properties like high transparency for a visible light or high thermal conductivity which are promising for future applications. When doped with boron, a p-type conductivity appears. As the doping concentration exceeds $\sim 4.5 \times 10^{21} \text{cm}^{-3}$ the system becomes metallic and eventually superconducting, with an unexpectedly high critical temperature on the order of a few Kelvin. [1, 2, 3] The critical temperature depends on the method by which the sample was grown.

Samples are most often prepared in thin layers, using the Microwave Plasma-assisted Chemical Vapour Deposition (MPCVD) method with growth orientations 100 and 111; see [4] and [5] respectively. The 111 samples have higher T_c than 100 samples. There are also bulk samples prepared with the High-Pressure High-Temperature (HPHT) method [6] with T_c comparable to the 100 samples. Some experimental data are collected in Fig. 5 below.

While the concentration of impurities is well under control in any of the above preparation methods, a concentration of binary correlations between

Email address: sopik@fzu.cz (Břetislav Šopík)

boron atoms is not and may cause the difference between samples. Here we discuss an effect of these correlations on T_c .

Our study is motivated by previous experimental studies. From the Raman scattering interpreted with the help of first-principle calculations Bourgeois *et al* suggested that boron atoms in boron-doped diamond form correlated multi-boron complexes, primarily dimers. [7] This is confirmed by Mukuda *et al* who observed a strong NMR line of isolated boron impurities in 111 samples, while this line is rather weak in 100 samples. [8]

We will assume that boron atoms tend to form isolated dimers but not large clusters. This assumption is supported by *ab initio* investigations which show that the nearest-neighbour dimer is the most favourable of all two-boron configurations while an added third boron tends to remain unassociated with the dimer [9, 10].

A dimer can be viewed as a molecule with bonding and anti-bonding states made of symmetric and anti-symmetric combinations of bound states of composing boron atoms. The symmetric state is deeper in the band gap than the boron state, therefore it does not contribute to N_0 , the density of states at the Fermi energy. [11, 7, 3] The energy of anti-symmetric states is above the isolated boron level and also does not contribute to N_0 . The formation of dimers thus reduces T_c .

To be able to perform numerically demanding configurational averaging within the Dynamical Cluster Approximation (DCA), we use a model which excludes many realistic features. We assume a simple cubic lattice with a single s-state per site, which does not cover the triple degeneracy of impurity state of boron [12]. The impurity potential is restricted to a single site having no long-range Coulomb tails, and eventual screening of this potential is not assumed. This model was already studied by Shirakawa *et al* [13] within the BCS theory, using the Coherent Potential Approximation for disorder, and also studied by one of the present authors [14] in the DCA for uncorrelated boron distribution.

The DCA allows us to include statistical weight of boron complexes given by their binary correlations. Nearest-neighbour positions of two boron atoms are favoured by a dimerization energy. To avoid large clusters, we assume that once the atom is in a dimer it cannot gain the dimerization energy from another neighbouring atom. For this model we evaluate the density of states on the Fermi level as a function of boron concentration and dimerization energy. The T_c is then obtained from the McMillan formula.

The paper is organized as follows. In section 2 we introduce the model Hamiltonian and describe the theory. In section 3 we calculate the density of states (DOS) and study the impact of boron correlations on N_0 . In section 4 we compare our theoretical values of the critical temperature with experimental data. Section 5 contains conclusions.

2. Theory

The presence of boron impurities at concentrations reaching 5% of the crystal atoms modify many properties of the crystal ranging from the lattice constant,

over the phonon spectrum and electron-phonon coupling, to the dielectric function. We neglect all these effects on superconductivity and express material parameters of McMillan formula as a function only of the density of states at the Fermi level N_0 . We introduce a model Hamiltonian and a method to calculate the density of states. At the end of this section we specify the probability distribution of boron clusters.

2.1. McMillan formula

The McMillan formula [15] provides the critical temperature

$$T_c = \frac{\hbar\omega_D}{1.45 k_B} \exp \left[- \frac{1.04(1 + \lambda)}{\lambda - \mu^*(1 + 0.62\lambda)} \right]. \quad (1)$$

Since the disorder-dependence of the Debye frequency in the boron-doped diamond is weak, we use the pure-diamond value $\hbar\omega_D/k_B = 1860$ K.

The screened pseudopotential

$$\mu^* = VN_0 \left[1 + VN_0 \ln \frac{E_C}{0.62\hbar\omega_D} \right]^{-1} \quad (2)$$

is given by the strength of the Coulomb interaction V . We have found neither measurement nor estimate of V in the literature, therefore we set this parameter from experimental T_c . A single value $V = 3.6 \times 10^{-23} \text{cm}^3 \text{eV}$ is used for all samples independently of boron concentration and correlation.

We estimate the Coulomb cutoff energy as

$$E_C = \frac{1}{2} N_0 \left(\frac{\partial N_E}{\partial E} \Big|_{E=0} \right)^{-1}. \quad (3)$$

For free particles this formula gives $E_C \rightarrow \hbar^2 k_F^2 / 2m$, usually used for the cutoff in metals [16]. In the impurity band the Fermi momentum k_F is not well-defined, but expression (3) in terms of the density of states is applicable. Since the Coulomb cutoff is only a subsidiary quantity, we use its uncorrelated value also for correlated samples. The concentration dependence must be maintained as one can see from the free-particle limit.

The electron-phonon coupling λ we take from *ab initio* calculations. The published results cover only a few concentrations, therefore we interpolate them in the spirit of the Morel-Anderson [17] formula

$$\lambda = \frac{UN_0}{1 + QN_0}. \quad (4)$$

Here U represents a phonon-electron coupling strength and QN_0 describes a screening.

Using formulae (1)-(4) we obtain T_c as a function of the density of states N_0 and its derivative giving the Coulomb cutoff E_C . The N_0 depends on the boron

concentration and dimerization energy. The E_C we take as a function of only the concentration.

In [14] it was shown that the Belitz theory with neglected vertex corrections provides a better agreement with data on 100 samples than the McMillan formula. For impurity concentrations up to 5% both approaches provide comparable results. In this paper we thus use the McMillan formula which is the standard approximation.

2.2. Density of states

Now we specify a model from which we obtain the density of states of non-interacting electrons as a function of the boron concentration n_B . It is given by a Hamiltonian of the valence band in diamond $\hat{\mathcal{H}}_0$ and a random potential of boron impurities $\hat{\mathcal{V}}$,

$$\hat{\mathcal{H}} = \hat{\mathcal{H}}_0 + \hat{\mathcal{V}} = \hat{\mathcal{H}}_0 + \sum_i \eta_i \delta \hat{a}_i^\dagger \hat{a}_i, \quad (5)$$

where $\eta_i = 1$ at impurity sites and zero elsewhere, and δ is the potential amplitude.

We employ the DCA for clusters of $2 \times 2 \times 2$ atoms on a cubic lattice. We only briefly introduce the DCA here; all details can be found in a previous paper of one of the authors [14] or in the method's original paper [18]. The DCA provides a Green function averaged over all possible configurations of impurities on a cluster embedded in an effective medium. The key point is how to close the self-consistency constructing the effective medium from the averaged Green function.

Naïve constructions based on a tight-binding representation of the self-energy have turned out to violate analytic properties and thus causality. In the DCA the self-energy is approximated in the momentum representation. The Brillouin zone is according to the size of the cluster divided into subzones – in our case $2 \times 2 \times 2$ subzones. Within these subzones the self-energy is momentum-independent; that is, the selfenergy is represented by eight complex functions of frequency.

All subzones contribute to the bare density of states

$$\rho^0(E) = \sum_{\mathbf{K}} \rho_{\mathbf{K}}^0(E), \quad (6)$$

where \mathbf{K} is a subzone index. In general, the subzone contribution $\rho_{\mathbf{K}}^0$ is obtained by integrating over the subzone with the electron dispersion of the valence band. For simplicity we approximate $\rho_{\mathbf{K}}^0$ in each subzone \mathbf{K} by a semielliptical function

$$\rho_{\mathbf{K}}^{(0)}(E) = \frac{1}{N_c} \frac{2}{\pi w_{\mathbf{K}}} \sqrt{1 - \left(\frac{E - E_{\mathbf{K}}}{w_{\mathbf{K}}} \right)^2}, \quad (7)$$

where N_c is number of subzones and

$$w_{\mathbf{K}} = \frac{1}{2}(E_{\mathbf{K}}^{\max} - E_{\mathbf{K}}^{\min}), \quad (8)$$

$$E_{\mathbf{K}} = \frac{1}{2}(E_{\mathbf{K}}^{\max} + E_{\mathbf{K}}^{\min}), \quad (9)$$

reproduce the maximum $E_{\mathbf{K}}^{\max}$ and minimum $E_{\mathbf{K}}^{\min}$ energy in the subzone \mathbf{K} .

The density of states (6) by definition maintains the width of the valence band. This approximation also yields a correct curvature at the edge; it correctly reproduces an effective mass of holes near the band edge. This feature is vital for a realistic description of the relatively shallow impurity state.

The parameters $w_{\mathbf{K}}$ and $E_{\mathbf{K}}$ are fitted to the tight-binding cosine band of width 22 eV. The impurity potential $\delta = 8.91$ eV reproduces the single-impurity bound state energy 0.37 eV above the valence band.

Each boron atom releases a single hole, therefore the density of holes equals n_B . From this density we determine the Fermi energy E_F

$$n_B = 2 \int_{E_F}^{\infty} \rho(E) dE. \quad (10)$$

Here the factor of two accounts for spin. After we find E_F we shift the energy reference point so that $E_F = 0$ as it is usual in the theory of superconductivity.

Mukuda *et al* [8] argued that the concentration of holes can differ from the boron concentration due to boron atoms in neutral B-H complexes or interstitial positions. On the other hand Klein *et al* [4] found that the effective number of carriers deduced from Hall-effect measurements was much larger than the number of boron atoms in samples. Since reliable hole concentrations are not accessible, we make the assumption that all samples are doped ideally.

2.3. Boron correlations

The exact form of boron correlations in the diamond remains a matter of discussion. We introduce their attractive correlation via an interaction energy ε_{dim} between boron atoms located at the nearest neighbour sites.

Let \mathcal{I} be a configuration of $n_{\mathcal{I}}$ boron atoms on N sites of the cluster with $q_{\mathcal{I}}$ boron pairs in nearest neighbour sites. Its probability

$$p_{\mathcal{I}} = \frac{1}{Z} x^{n_{\mathcal{I}}} (1-x)^{N-n_{\mathcal{I}}} e^{-q_{\mathcal{I}} \frac{\varepsilon_{\text{dim}}}{k_B T_p}} \quad (11)$$

is given by a configuration statistical factor and by total energy scaled by the temperature of sample preparation T_p . Typical T_p for 100 and 111 samples is about 1100 K. The probability is normalized to unity, $\sum_{\mathcal{I}} p_{\mathcal{I}} = 1$, which determines Z . The parameter x determines to the boron concentration

$$n_B = \sum_{\mathcal{I}} n_{\mathcal{I}} p_{\mathcal{I}}. \quad (12)$$

For uncorrelated boron atoms, $\varepsilon_{\text{dim}} \rightarrow 0$, it equals the boron concentration, $x \rightarrow n_B$. In our case $N = 8$ which allows for 2^8 configurations. By symmetry one can reduce a number of configurations which must be treated numerically.

Apparently, averaging over small clusters underestimates contribution of dimers. In the simplest case of $1 \times 1 \times 1$ cluster the dimers are absent. In the assumed case of $2 \times 2 \times 2$ all atoms are on the surface of the cluster with half of nearest neighbors in the cluster and half outside. The outer neighbors are not accounted for which reduces the effect of dimers crudely by half. It can be partly compensated by an artificial increase of the dimerization energy by $\varepsilon_2 = -k_B T_p \ln 2$.

3. Density of states in the presence of boron dimers

Energy levels of a boron dimer are rather distinct from a level of an isolated atom. While a hole binds to an isolated atom at 0.37 eV, for our model the dimer has the symmetric level at 1.6 eV and the anti-symmetric state forms only a resonant level in the valence band at -2.2 eV. For majority of samples the boron concentration is less than 5%, therefore isolated boron atoms prevail in uncorrelated configurations. When the energy gain of two boron atoms at neighbour positions exceeds the preparation temperature, $\varepsilon_{\text{dim}} \gg K_B T_p \sim 94.8$ meV, the fraction of dimers becomes large and this modifies the spectrum of energies in the sample.

The effect of boron dimers on the overall density of states in the impurity band for 5% boron doping is shown in Fig. 1, where we compare the DOS for uncorrelated case a) with two correlated cases. In the case b) we take the boron-boron binding energy $\varepsilon_{\text{dim}} = -160$ meV resulting from *ab initio* calculations [7, 9, 10]. We refer to this binding energy as a *realistic correlation*. In the case c) we use binding energy $\varepsilon_{\text{dim}} = -460$ meV which yields the best fit of experimental data, see comparison in Fig. 5. We shall refer to this binding energy as a *fitted correlation*.

It should be noted that *ab initio* studies compare energies of periodic crystals made of clusters B_2C_{62} or B_2C_{52} with selected configuration of boron atoms. Energies which one can interpret as the binding energy of a nearest neighbour dimer achieve values ranging from -158 meV, over -205 meV to -288 meV depending on authors and eventual gradient corrections. The fitted correlation energy -460 meV is thus not far from these values.

We focus on the impurity band because the Fermi energy, $E_F = 0$, lies there. The shape of the valence band is unimportant as it extends over energy interval from -1.5 eV to -24.5 eV. The thick line represents the density of states and thin lines are its decomposition into contributions according to number of boron atoms in the $2 \times 2 \times 2$ cluster. All configurations of n boron atoms are added together so that they contribute with probability $p_n = \sum_{\mathcal{I}}^{n_{\mathcal{I}}=n} p_{\mathcal{I}}$.

Probabilities of n -boron clusters for the uncorrelated case are $p_0 = 0.66$, $p_1 = 0.28$ and $p_2 = 0.05$. The zero-boron clusters contribute mainly to the valence band. In the impurity band they give a small contribution due to states tunneling from the surrounding medium. States from the single-boron clusters dominate the impurity band.

The two-boron clusters include 12 nearest-neighbour configurations which are the dimers, 12 from second-nearest neighbours, and four from third-nearest

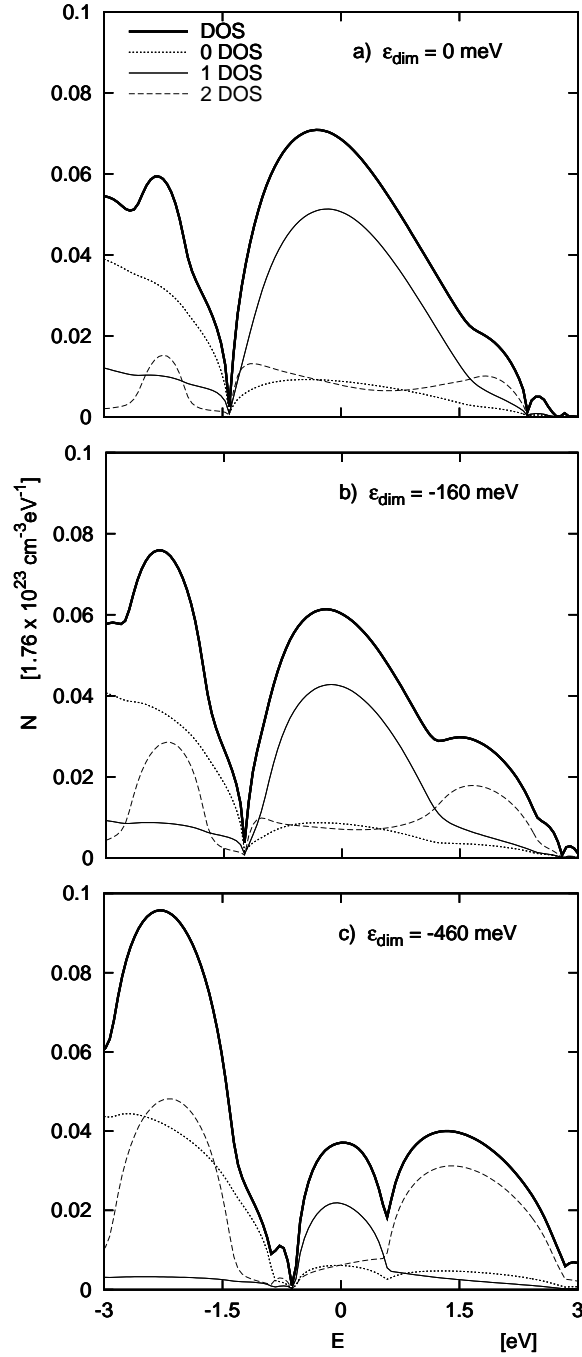


Figure 1: Density of states at doping $n_B = 0.05$. Positions of boron atoms at neighbour sites are a) uncorrelated b) correlated by energy $\epsilon_{\text{dim}} = -160$ meV found from realistic *ab initio* studies and c) correlated by $\epsilon_{\text{dim}} = -460$ meV fitted to give best agreement with experimental data. The growth temperature is $T_p = 1100$ K. Thick line represents the DOS and thin lines its decomposition into contributions according to number of boron atoms in the $2 \times 2 \times 2$ cluster.

neighbours. For uncorrelated system in Fig. 1a) the dimers increase the DOS at the upper edge of the impurity band around $E \sim 1.55$ eV, and in the valence band at $E \sim -2.15$ eV. In the correlated cases in Fig. 1b) and c) their contribution is even more pronounced. The position of the two-boron levels are shifted due to an increase of the dimer fraction in two-boron clusters and due to feedback effect of surrounding medium.

The small split band near $E = 2.4$ eV in uncorrelated case in Fig. 1a) is due to three-boron complexes. For realistic correlations it shifts towards higher energies. For fitted correlations it merges with the main impurity band. States of clusters with more boron atoms are also present, but their contributions are very small for the given concentration.

The realistic correlated case b) differs from the uncorrelated one a) mainly in the probability of zero-, single-, and double-boron cluster contributions. For given binding energy $\varepsilon_{\text{dim}} = -160$ meV they are $p_0 = 0.70$, $p_1 = 0.21$ and $p_2 = 0.08$. In accordance with decreased p_1 and increased p_2 , the contributions of double and higher boron states are enhanced and the peak associated with single boron states is reduced. The lower probability of the single-boron clusters leads to the decrease of the DOS at the Fermi energy.

With fitted correlation c) the contributions from larger clusters of boron atoms become more apparent. For $\varepsilon_{\text{dim}} = -460$ meV we find $p_0 = 0.77$, $p_1 = 0.07$ and $p_2 = 0.15$, therefore the number of boron atoms in dimers is four times higher than the number of isolated atoms. As one can see in Fig. 1c) the major part of the impurity band is due to dimer states.

Note that even when dimers dominate, the Fermi energy remains in the single-atom part of the impurity band. This follows from the fact that each dimer binds two holes of spin up and down in the symmetric state. Since the number of boron atoms in dimers equals the number of bounded holes, two boron donors become passivated when they form a dimer. The metallic band is thus formed only by unpaired boron atoms.

The dimers influence the density of states in two ways. First, they effectively reduce the doping level. Second, they contribute to the medium in which the band is formed. To demonstrate the second effect in Fig. 2 we have included a DOS for uncorrelated system with $n_B = 0.0091$ giving the probability of single-atom clusters $p_1 = 0.07$ being equal to p_1 of the fitted correlation. One can see that the approximation of a correlated system by a non-correlated one with dimers subtracted from the boron concentration leads to correct shape of the metallic band except for the contribution of clusters with dimers to the density of states at the Fermi level. For parameters in Fig. 2 this contribution is a significant $\sim 20\%$, assuming exponential dependence of T_c on N_0 .

The dependence of N_0 on the strength of boron correlations is shown in Fig. 3. One can see that positive correlations in boron distribution lower the density of states at the Fermi level N_0 for any doping n_B . Fig. 3 also presents the Coulomb cutoff given by formula (3). This value is very close to the distance of the Fermi level from the right band edge. An alternative definition of the Coulomb cutoff from the bad edge, however, is imposed due to split off bands of trimers and larger clusters of low probability.

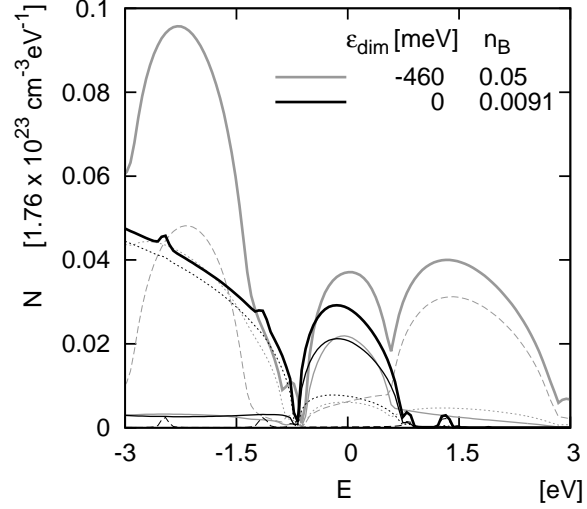


Figure 2: Approximation by subtracted dimers. The density of states at doping $n_B = 0.05$ and fitted correlation $\epsilon_{\text{dim}} = -460$ meV (gray re-plot from Fig. 1c) is compared with uncorrelated system of concentration $n_B = 0.0091$ (in black lines). Both systems have the same probability of single-boron clusters giving similar 1DOS (thin line). They have also similar 0DOS (dotted lines). The single-boron states, however, easily tunnel into two-boron clusters giving appreciably larger contribution of 2DOS (dashed lines) at the metallic band.

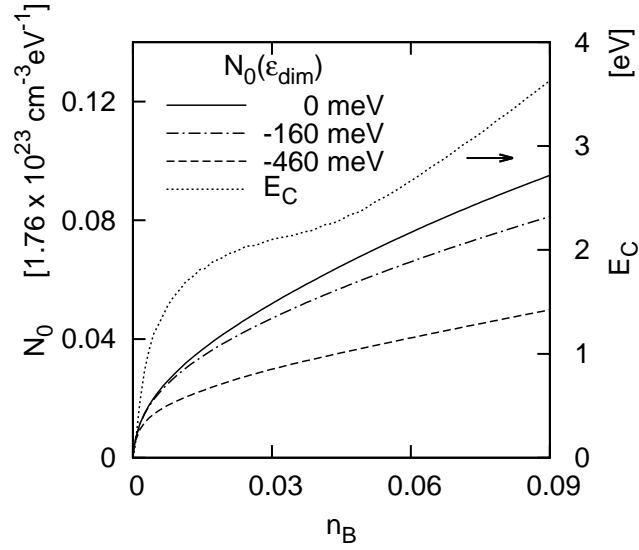


Figure 3: The density of states at the Fermi energy N_0 as a function of boron concentration n_B for no (full line), realistic (dashed-dot line) and fitted (dashed line) correlation. The left vertical axis corresponds to the Coulomb cutoff E_C (dotted line) evaluated for uncorrelated boron atoms.

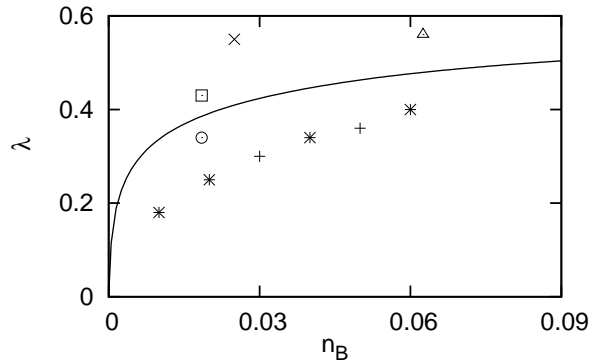


Figure 4: Coupling constant λ as a function of the boron concentration. Symbols represent results of *ab initio* calculations of λ for uncorrelated boron-doped diamond. Solid line reproduces λ dependence on n_B using formula (4) with uncorrelated $N_0(n_B)$ (see Fig. 3) and parameters $Q = 35.7 \times 10^{-23} \text{cm}^3 \text{eV}$, $U = 23.3 \times 10^{-23} \text{cm}^3 \text{eV}$. *Ab initio* results were obtained within the Virtual Crystal (+ [19], × [20], * [21]) and Super Cell (□ [22], △ [23], ○ [24]) method.

4. Dependence of critical temperature on boron correlations

Now we are ready to discuss the impact of correlations on T_c . We ask the question whether different T_c of the 100 and 111 samples can be explained by a different content of dimers. Mukuda *et al* [8] have observed a strong NMR line of single-boron state in the 111 samples while this line was rather weak in the 100 samples. Based on this experimental fact we treat 111 samples as uncorrelated while in the 100 and HPHT samples we include dimers.

First we specify material parameters. The Q and U are chosen to reproduce *ab initio* calculations of coupling parameter λ in uncorrelated boron-doped diamond. Formula (4) with uncorrelated $N_0(n_B)$ and parameters $Q = 35.7 \times 10^{-23} \text{cm}^3 \text{eV}$ and $U = 23.3 \times 10^{-23} \text{cm}^3 \text{eV}$ is compared with *ab initio* values in Fig. 4. Values V and ε_{dim} are not accessible in print, we thus fit them to experimental values of T_c . The best agreement is achieved for $V = 3.6 \times 10^{-23} \text{cm}^3 \text{eV}$ and $\varepsilon_{\text{dim}} = -460 \text{meV}$.

In Fig. 5 we compare T_c from McMillan formula (1) for uncorrelated and correlated systems with experimental data for 111, 100 and HPHT samples. As one can see the realistic correlation energy $\varepsilon_{\text{dim}} = -160 \text{meV}$ found in *ab initio* studies is too low to explain differences in the critical temperature. With the fitted correlation energy $\varepsilon_{\text{dim}} = -460 \text{meV}$, the theory reproduces trends of experimental values for small concentrations. For $n_B > 0.02$ one finds only qualitative agreement.

Compared to the experimental data, the present study underestimates the difference between 111 and 100 samples. It can be in part due to our simple model, in part due to approximations employed to evaluate the density of states. First of all, inside the $2 \times 2 \times 2$ cluster each atom has only three nearest neigh-

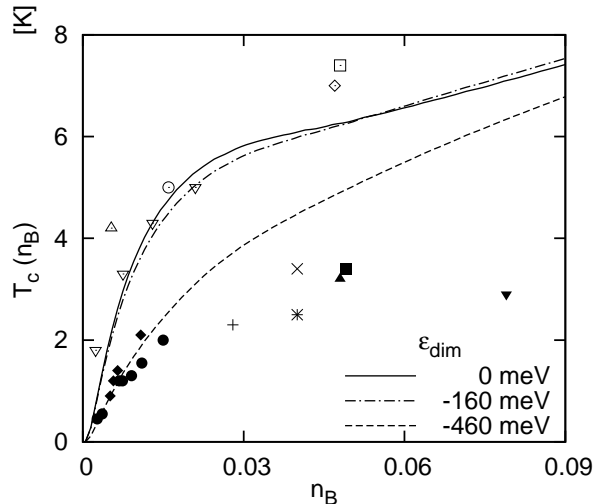


Figure 5: Critical temperature T_c as a function of boron doping for no (solid line), realistic (dashed-dot line), and fitted correlation (dashed line). Open symbols represent 111 MPCVD data (\square [5], \diamond [6], \circ [8], \triangle [25], ∇ [26]), full symbols 100 MPCVD data (\bullet [4], \blacktriangle [5], \blacksquare [8], \blacklozenge [27], \blacktriangledown [28]) and crosses HPHT samples ($+$ [1], \times [29], $*$ [30]).

hours while in the crystal it has six. Accordingly, each boron can form only three dimers inside the cluster while three dimers cross the cluster border. The correlations corresponding to the former are covered in our treatment while those corresponding to the latter are not.

There are also additional mechanisms that appear already in our model but have not been included for simplicity of discussion. For example, two boron atoms at second-neighbour positions form a symmetric state of energy 0.91 eV which is close to the single-atom bound state and at concentrations above 1% contributes to the metallic band. The anti-symmetric state of such a boron pair has energy at -0.8 eV which forms a resonant level in the valence band and does not contribute to the impurity band. One can crudely say one half of boron atoms in the second-neighbour dimers are passivated.

5. Conclusion

In this paper we have addressed the impact of correlations of boron impurities on the density of states and thus on the critical temperature T_c of the superconducting transition. To this end we have calculated the impurity-band density of states for several strengths of attractive correlations between boron atoms. Calculations have been done within a one-band cubic lattice with on-site impurity model employing the DCA method on a cluster of $2 \times 2 \times 2$ atoms.

We have found that correlations enhance states associated with multi-boron complexes reducing the density of states at the Fermi energy, see Fig. 1 and

Fig. 3. Following NMR data we have approximated 111 oriented samples as an uncorrelated system and 100 samples as a system with correlations. We have found that an *ab initio* binding energy $\varepsilon_{\text{dim}} = -160$ meV of boron dimer is not sufficient to explain differences in T_c . From the best fit we have found the binding energy $\varepsilon_{\text{dim}} = -460$ meV which explains experimental data at least for boron concentrations below 2%.

The studied model has several shortcomings. It has overly-simplified electronic band structure and the binding potential is single-site. Also our treatment of the disorder covers only contributions of boron complexes to the density of states but neglects other disorder effects like the weak localization, which has been discussed as a possible mechanism enhancing the superconductivity. [31] Nevertheless, our results strongly indicate that binary correlations are responsible for different critical temperatures of the 111 and 100 samples.

Authors would like to thank Jiří Mareš and Jan Mašek for many useful discussions and also Peter Matlock for careful reading of a manuscript. The access to the METACentrum supercomputing facilities provided under the research plan MSM6383917201 is also highly appreciated. This work was supported by research plans MSM0021620834 and No. AVOZ10100521, by grants, GAČR P204/10/0687, GAČR P204/10/0212 and DAAD project.

References

- [1] E. A. Ekimov, V. A. Sidorov, E. D. Bauer, N. N. Mel'nik, N. J. Curro, J. D. Thompson, and S. M. Stishov, *Nature*, **428**, 542 (2004).
- [2] E. Bustarret, *physica status solidi (a)*, **205**, 997 (2006).
- [3] X. Blase, E. Bustarret, C. Chapelier, T. Klein, and C. Marcenat, *Nature materials*, **8**, 375 (2009).
- [4] T. Klein, P. Achatz, J. Kacmarcik, C. Marcenat, F. Gustafsson, J. Marcus, E. Bustarret, J. Pernot, F. Omnes, B. E. Sernelius, C. Persson, A. F. da Silva, and C. Cytermann, *Physical Review B*, **75**, 165313 (2007).
- [5] Y. Takano, T. Takenouchi, S. Ishii, S. Ueda, T. Okutsu, I. Sakaguchi, H. Umezawa, H. Kawarada, and M. Tachiki, *Diamond and Related Materials*, **16**, 911 (2007).
- [6] T. Yokoya, T. Nakamura, T. Matsushita, T. Muro, Y. Takano, M. Nagao, T. Takenouchi, H. Kawarada, and T. Oguchi, *Nature*, **438**, 647 (2005).
- [7] E. Bourgeois, E. Bustarret, P. Achatz, F. Omnès, and X. Blase, *Physical Review B*, **74**, 094509 (2006).
- [8] H. Mukuda, T. Tsuchida, A. Harada, Y. Kitaoka, T. Takenouchi, Y. Takano, M. Nagao, I. Sakaguchi, T. Oguchi, and H. Kawarada, *Physical Review B*, **75**, 033301 (2007).

- [9] R. Long, Y. Dai, M. Guo, L. Yu, B. Huang, R. Zhang, and W. Zhang, *Diamond and Related Materials*, **17**, 234 (2008).
- [10] L. Niu, J.-Q. Zhu, X. Han, M.-L. Tan, W. Gao, and S.-Y. Du, *Physics Letters A*, **373**, 2494 (2009).
- [11] J. P. Goss and P. R. Briddon, *Physical Review B*, **73**, 085204 (2006).
- [12] Y. G. Pogorelov and V. M. Loktev, *Phys. Rev. B*, **72**, 075213 (2005).
- [13] T. Shirakawa, S. Horiuchi, Y. Ohta, and H. Fukuyama, *Journal of the Physical Society of Japan*, **76**, 014711 (2007).
- [14] B. Šopík, *New Journal of Physics*, **11**, 103026 (2009).
- [15] W. L. McMillan, *Phys. Rev.*, **167**, 331 (1968).
- [16] S. V. Vonsovsky, Y. A. Izyumov, and E. Z. Kurmaev, *Superconductivity of Transition Metals Their Alloys and Compounds* (Springer-Verlag Berlin Heidelberg, Germany, 1982).
- [17] P. Morel and P. W. Anderson, *Phys. Rev.*, **125**, 1263 (1962).
- [18] M. Jarrell and H. R. Krishnamurthy, *Phys. Rev. B*, **63**, 125102 (2001).
- [19] L. Boeri, J. Kortus, and O. K. Andersen, *Phys. Rev. Lett.*, **93**, 237002 (2004).
- [20] K.-W. Lee and W. E. Pickett, *Phys. Rev. Lett.*, **93**, 237003 (2004).
- [21] Y. Ma, J. S. Tse, T. Cui, D. D. Klug, L. Zhang, Y. Xie, Y. Niu, and G. Zou, *Phys. Rev. B*, **72**, 014306 (2005).
- [22] X. Blase, C. Adessi, and D. Connétable, *Phys. Rev. Lett.*, **93**, 237004 (2004).
- [23] H. J. Xiang, Z. Li, J. Yang, J. G. Hou, and Q. Zhu, *Phys. Rev. B*, **70**, 212504 (2004).
- [24] F. Giustino, J. R. Yates, I. Souza, M. L. Cohen, and S. G. Louie, *Physical Review Letters*, **98**, 047005 (2007).
- [25] Y. Takano, M. Nagao, I. Sakaguchi, M. Tachiki, T. Hatano, K. Kobayashi, H. Umezawa, and H. Kawarada, *Applied Physics Letters*, **85**, 2851 (2004).
- [26] Y. Takano, M. Nagao, T. Takenouchi, H. Umezawa, I. Sakaguchi, M. Tachiki, and H. Kawarada, *Diamond and Related Materials*, **14**, 1936 (2005).
- [27] E. Bustarret, J. Kačmarčík, C. Marcenat, E. Gheeraert, C. Cytermann, J. Marcus, and T. Klein, *Phys. Rev. Lett.*, **93**, 237005 (2004).

- [28] H. Umezawa, T. Takenouchi, Y. Takano, K. Kobayashi, M. Nagao, I. Sakaguchi, M. Tachiki, T. Hatano, G. Zhong, M. Tachiki, and H. Kawarada, (2005).
- [29] V. A. Sidorov, E. A. Ekimov, S. M. Stishov, E. D. Bauer, and J. D. Thompson, *Phys. Rev. B*, **71**, 060502 (2005).
- [30] V. Sidorov, E. Ekimov, E. Bauer, N. Mel'nik, N. Curro, V. Fritsch, J. Thompson, S. Stishov, A. Alexenko, and B. Spitsyn, *Diamond and Related Materials*, **14**, 335 (2005).
- [31] J. Mareš, M. Nesládek, P. Hubík, D. Kindl, and J. Krištofik, *Diamond and Related Materials*, **16**, 1 (2007).